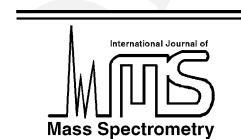




ELSEVIER

International Journal of Mass Spectrometry 12237 (2002) 1–12



www.elsevier.com/locate/ijms

Trace gas monitoring at the Mauna Loa Baseline Observatory using Proton-Transfer Reaction Mass Spectrometry

Thomas Karl^{a,*}, Armin Hansel^b, Tilmann Märk^b, Werner Lindinger^b, David Hoffmann^c

^a National Center for Atmospheric Research, Atmospheric Chemistry Division, P.O. Box 3000, Boulder, CO 80307, USA

^b Institute for Ion Physics, University of Innsbruck, Innsbruck, Austria

^c Climate Monitoring and Diagnostics Laboratory, National Oceanographic and Atmospheric Administration, Boulder, CO, USA

Received 14 March 2002; accepted 7 June 2002

Abstract

Real time monitoring of volatile organic compounds (VOCs) using a Proton-Transfer Reaction Mass Spectrometer was performed at the Mauna Loa Baseline Station (19.54N, 155.58W) in March/April 2001 (March 23, 2001–April 17, 2001). Mixing ratios for methanol, acetone, acetonitrile, isoprene and methyl vinyl ketone (MVK) plus methacrolein (MACR) ranged between 0.2 and 1.8, 0.2 and 1, 0.07 and 0.2, <0.02 and 0.3, and <0.02 and 0.5 ppbv, respectively. Biomass burning plumes transported from South-East Asia and the Indian Subcontinent across the Pacific influenced part of the measurement campaign. Δ Acetonitrile/ Δ CO and Δ acetone/ Δ acetonitrile ratios in these cases were 1.5×10^{-3} to 2.5×10^{-3} and 2–5 ppbv/ppbv, respectively. Overall Asian outflow events were not as frequent during Spring 2001 as in previous years. Methanol did not show significant correlation with CO, acetonitrile, and acetone. The abundance of acetone and CO seemed to be influenced but not dominated by biomass burning and domestic biofuel emissions. (Int J Mass Spectrom, in press)

© 2002 Published by Elsevier Science B.V.

Keywords: Trace gas monitoring; Proton-Transfer Reaction Mass Spectrometry; Volatile organic compounds

1. Introduction

Taking into account the expected economic expansion around the Pacific Rim and in the rest of the world, it becomes obvious that pollution can be delivered across the Pacific unless preventative measures are taken. Sharma et al. [1] reported high concentrations of nonmethane-hydrocarbons (NMHC) at Oki Island in Japan and concluded that the East Asia Pacific Rim Region is significantly contaminated from anthropogenic emission transported from the Asian continent by rapid convective movement of air masses.

Detailed trajectory analysis by Newell and Evans [2] revealed the seasonal patterns of trans-Pacific transport and the relative importance of Asian and European sources. Polluted air in springtime is typically lifted to the upper troposphere and subsequently transported across the Pacific by the aloft. About 40% of the backtrajectories arriving at the Climate Monitoring and Diagnostics Laboratory (CMDL) monitoring station on Mauna Loa in Spring point westwards and indicate fast ‘outflowing’ Asian air masses [3]. The pan-Pacific air quality problem has recently been impressively demonstrated by satellite remote sensing images of trans-Pacific aerosol transport in April 1998 and March 2001 [3,4]. MOPITT (Measurements

* Corresponding author. E-mail: tomkarl@ucar.edu

of Pollutants in the Troposphere) data revealed substantial export of CO from South-East Asia due to biomass burning activity in this region in Spring 2000 [50]. Singh et al. [5] published results of several abundant oxygenated volatile organic compounds (VOCs) in the Southern and Northern Pacific Hemisphere. The authors concluded that current atmospheric global models are incapable of reproducing ambient mixing ratios of several oxygenated species such as methanol, acetaldehyde, and acetone. The latter three compounds account for more than 65% of the total VOC loading at remote places, such as the Southern Indian Ocean [6,7]. These compounds play an important role in the oxidant balance of the troposphere. Recent evidence suggests that on a global basis acetaldehyde, methanol, and acetone contribute to the “large, diffuse and hitherto-unknown sources of oxygenated organic compounds” seen in the atmosphere [5]. Results from the Indian Ocean Experiment (INDOEX) [6,8–10] demonstrated the importance of biofuel on the Asian Subcontinent. Wisthaler et al. [6] measured the relative abundance of acetonitrile, which represents a selective tracer for biomass burning, to CO suggesting a strong biomass burning source in West India. Similar results were obtained by de Gouw et al. [9]. Results from the Trace P (Transport and Chemical Evolution over the Pacific) experiment show significant pollution off the coast of East Asia and suggest transport of polluted layers into the Pacific. In this paper, we present measurements of methanol, acetonitrile, acetone, isoprene, and methyl vinyl ketone (MVK) plus Methacrolein (MACR), measured by Proton-Transfer Reaction Mass Spectrometry (PTR-MS) at the Mauna Loa Baseline Station during Spring 2001.

2. Experimental

The PTR-MS instrument was situated inside the Keeling building of the CMDL network station on Mauna Loa. Air was pulled through a 10-m manifold (i.d. 10 cm) down from the top of the sampling tower at a pumping speed of ~ 300 L/s. The pressure inside the manifold was approx. 640 mbar. A 5-m PFA-line (i.d.

1/8 in.) pumped by a diaphragm pump (Pfeiffer, MD4) at a pumping speed of 30 L/min was used to bypass part of this air stream into the PTR-MS sampling line. At its end, another bypass (i.d. 1/16 in.) led 15 sccm into the PTR-MS instrument. The pressure in the 5-m sampling line was reduced down to 400 mbar in order to avoid condensation inside the building, minimize memory effects and assure a fast response time. The overall delay time was less than 5 s. Leak tests were performed with methanol using the fast monitoring capabilities of the PTR-MS.

The Proton-Transfer Reaction Mass Spectrometer has been described in detail elsewhere [11]. H_3O^+ ions are used to ionize VOC via proton-transfer reactions. Since any VOC having a higher proton affinity than water can be ionized by H_3O^+ , reported concentrations have to be regarded as upper limits. However, as demonstrated, potential interferences for several VOCs (such as acetonitrile, acetone, and methanol) are either very small (e.g., propanal on mass 59⁺) or nonexistent [12,13]. The value for E/N (E being the electric field strength and N the buffer gas density) in the drift tube was kept at about 123 Townsend (Td) high enough to avoid strong clustering of H_3O^+ ions with water and thus a humidity-dependent sensitivity. The sensitivity of the PTR-MS instrument during the Mauna Loa field study was typically on the order of 140 Hz/ppbv (counts per second per ppbv) for acetone and 64 Hz/ppbv for methanol at 2.3 mbar buffer gas pressure with a reaction time of 110 μs and 4 MHz H_3O^+ ions and was obtained from a calibration standard as well as from the theoretical first order reaction:

$$\text{H}_3\text{O}^+ + \text{VOC} \xrightarrow{k} \text{VOCH}^+ + \text{H}_2\text{O}, \quad (1)$$

with k being the reaction rate constant. The detection limit (DL) for compounds investigated in this work was inferred from a signal to noise ratio (S/N) of 2 according to $\text{DL} = 2 \times \text{S.D.}_{\text{blank}}/\text{sensitivity}$, with $\text{S.D.}_{\text{blank}}$ being the standard deviation of background countrates. For a 10-s integration time, this resulted in detection limits of 54, 6, 8, 10, and 10 pptv for methanol, acetonitrile, acetone, isoprene, and MVK + MACR, respectively. The uncertainty of the concentration measurement was $\pm 20\%$ according to the spec-

ifications of a high concentration standard used for calibration in this work. The PTR-MS was operated in a selective ion mode from March 23, 2001 until April 17, 2001 with a cycling rate of ~ 6 min. Reference measurements were taken through a catalytic converter (platinum wool at 430°C) and were performed about every 30 min to 2 h.

Meteorological data and various other atmospheric components, such as surface CO, CH₄, ozone, and halocarbons were available from continuous long-term measurements being made at the Mauna Loa station. Detailed backtrajectory analysis for Spring 2001 with data from the global ECMWF model were available from CMDL, NOAA (National Oceanic and Atmospheric Administration), and the HYSPLIT4 (Hybrid Single-Particle Lagrangian Integrated Trajectory) model [14].

3. Results

3.1. Meteorology

Long-range transport to the Mauna Loa Observatory (MLO) is governed mainly by the interplay of the northeasterly trades, the subtropical jet, the seasonal variation of the quasi-permanent North Pacific subtropical anticyclone and synoptic scale disturbances [15]. In Spring, the anticyclone starts to intensify and migrate northwest, which allows air masses to arrive at the MLO from Asia anticyclonically by curving in the last few days to the south and then west to Hawaii. This typical Spring pattern seemed to have mixed air masses coming from the East Pacific Rim Region south to the observatory on April 13–17. A synoptic scale disturbance shifted the large-scale flow from SE to NE on March 28–29 and caused north easterlies along with elevated pollutant concentrations on the subsequent three days (March 29–31). Spring is characterized by the highest frequency of Asian dust transport to Hawaii [16] and the time of maximum ozone concentrations at the observatory [17]. Indeed, around the second and third week in April 2001, a large dust storm originating from Inner Mongolia passed across

the North Pacific and migrated as far as the Mid-West of the US. Backtrajectory analysis suggests that part of these air masses, while crossing the Pacific, were mixed south to the MLO.

The local meteorological patterns at the site are mainly governed by the strength of synoptic-scale or trade winds, the height and strength of the trade wind inversion, the flow of the synoptic winds around the island mountain topography, and the daily heating and cooling cycle on the island. Daytime heating of the island causes a pronounced sea breeze circulation that can force surface air as far as 10 km inland [18]. The warmer land mass results in upslope winds, which typically reach a maximum during the early afternoon and mix boundary layer air up to the site. Afternoon upslope conditions can bring humid air (Fig. 1, panel 1) along with increased concentrations of some locally produced compounds (e.g., from the rain forest and/or ocean) to the observatory. Daytime upslope flow weakens after sunset. Winds become light and variable during the evening transition period. When the mountain has cooled sufficiently, dry downslope flow develops. Nighttime drainage winds dissipate a few hours after sunrise as a result of rapid surface heating. At mid-morning, turbulent upslope flow begins again and cumulus clouds usually form in the saddle region between Mauna Loa and Mauna Kea. At times, when the inversion is weak (approx. $+1^\circ\text{C}$), upslope winds can carry moist boundary layer air up to the observatory. The thickness of the surface layer at the site is approximately 600 m during upslope and 55 m during downslope conditions [19]. As discussed by Walega et al. [20], ozone exhibits a well-known afternoon minimum (Fig. 1, panel 2) due to low NO concentrations in the marine boundary layer in upslope flow.

3.2. Isoprene and MVK + MACR

Isoprene ($k_{\text{HO}}^{298} = 1 \times 10^{-10} \text{ cm}^3/\text{molecule s}$ [21]) and MVK + MACR (averaged $k_{\text{HO}}^{298} = 2.7 \times 10^{-11} \text{ cm}^3/\text{molecule s}$ [21]) were monitored at protonated masses 69^+ and 71^+ , respectively. These ions showed a very pronounced diurnal cycle with concentrations peaking in the afternoon during upslope conditions.

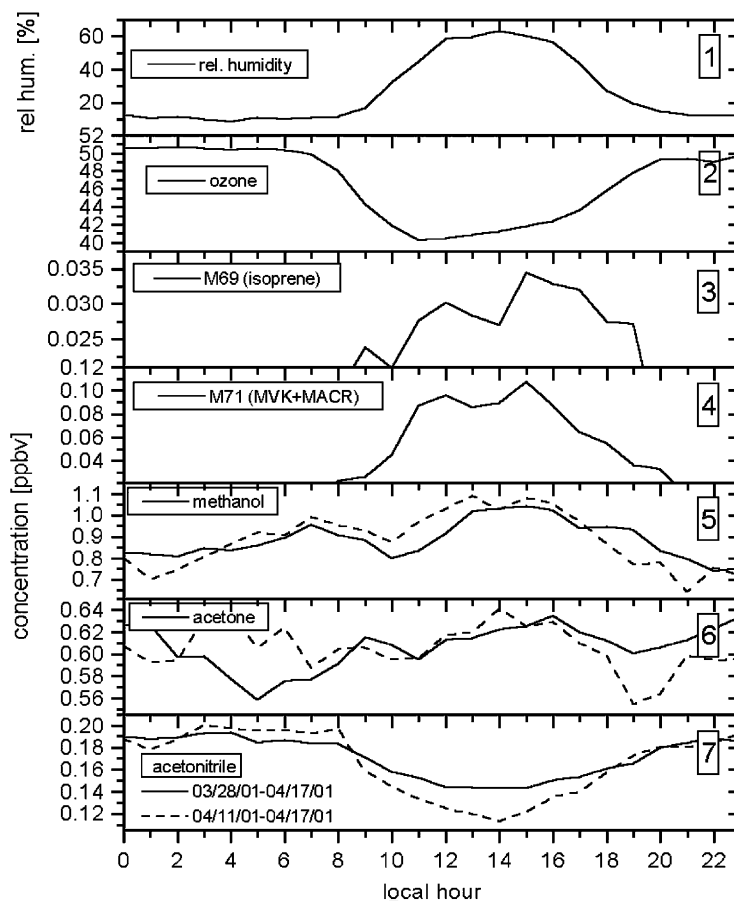


Fig. 1. Averaged diurnal variations of humidity [measured by the $(\text{H}_2\text{O})_2\text{H}_3\text{O}^+$ cluster], ozone, isoprene, MVK + MACR, methanol, acetone, and acetonitrile. Dashed curves in panels 5, 6, and 7 show the averaged diurnal cycle from April 11 till 17.

213 Nighttime concentrations were close to and below
 214 the detection limit <10 pptv. Several potential in-
 215 terferences exhibiting mass 69^+ have been reported
 216 [12,13]. For example, unsaturated C_5 -alcohols and
 217 C_5 -aldehydes, which can be released by freezing
 218 vegetation, dehydrate partially during proton transfer
 219 and thus interfere on mass 69^+ . In addition, Harley
 220 et al. [22] and Goldan et al. [23] reported that several
 221 North American pines release substantial amounts of
 222 a C_5 -alcohol, 2,3,2-methylbutenol (232-MBO), in a
 223 light- and temperature-dependent manner. These in-
 224 terferences cannot be excluded a priori and ambient
 225 concentrations for isoprene, therefore, represent an
 226 upper limit. Greenberg et al. [24] reported isoprene

227 concentrations around 4–46 pptv during the MLO
 228 Photochemistry Experiment 2 (MLOPEX 2). This is
 229 close to the mean upslope concentrations (~ 30 pptv)
 230 observed on mass 69^+ during this study. Fig. 1 (pan-
 231 els 3 and 4) shows the averaged diurnal variation of
 232 mass 69^+ (isoprene) and its oxidation products mass
 233 71^+ (MVK + MACR) during the 4-week measure-
 234 ment period. Isoprene is most likely emitted by local
 235 vegetation and brought up to the observatory by the
 236 diurnal land–sea breeze circulation. Milne et al. [25]
 237 reported that isoprene can be produced by phytoplank-
 238 ton and thus emitted by the ocean. Major biogenic
 239 interferences can be excluded due to the warm climate
 240 (no wound compounds due to temperatures below

freezing) and the local tropical vegetation, which does not accommodate MBO emitting species such as North American pine trees. Helmig et al. [26] investigated the presence of 86 organic species by detailed GC–FID and GC–MS analysis during the MLOPEX 2 study. None of the reported compounds (except isoprene) would contribute to the observed signal on mass 69⁺. On an average, two to three times higher mixing ratios of MVK + MACR were observed. Assuming that no significant interferences for the oxidation products of isoprene chemistry exist and taking OH densities on the order of 5×10^6 molecules/cm³ [27], we derive an average daytime photochemical age between emission and arrival at the observatory of roughly 48 min or a radius of 15 km at an average windspeed of 5 m/s. This is consistent with the idea that upslope winds transport these locally emitted compounds to the site.

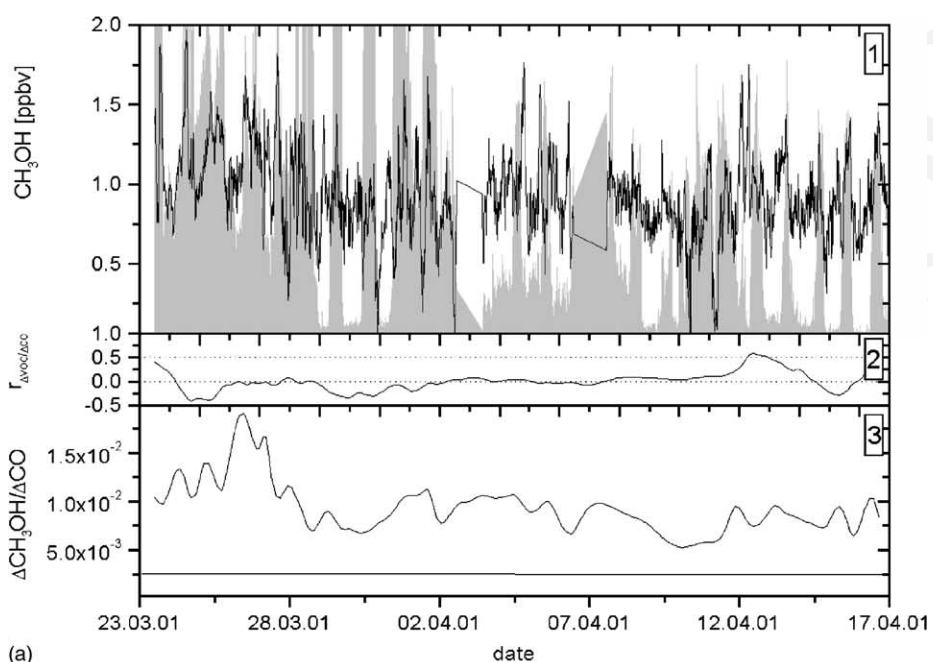
3.3. Methanol

Methanol showed concentrations between 0.2 and 1.8 ppbv, close to values (0.5 and 1.6 ppbv) measured by Wisthaler et al. [6] and Warneke and de Gouw [7] in the remote Indian Ocean. Average nighttime concentrations around 800 pptv were a little lower than reported by Singh et al. [5], who measured mean methanol concentrations around 900 pptv in the remote Pacific. The diurnal profile for methanol is shown in Fig. 1 (panel 5). Maximum concentrations were typically observed around 14:00 together with masses 69⁺, 71⁺, and humidity (measured by the second water cluster (H₂O)₂H₃O⁺). This suggests that methanol had local sources and was advected to the station by upslope winds. Correlation of methanol and CO was poor with correlation coefficients r between -0.4 and $+0.1$ in general, thus suggesting different origin (except for times when local pollution caused enhanced CO levels at the site by upslope winds, e.g., on April 12, 2001). Methanol to CO ratios are shown in Fig. 2a (panel 3). The straight line (Fig. 2a, panel 3) reflects an average emission factor ($\Delta\text{CH}_3\text{OH}/\Delta\text{CO} = 3.3 \times 10^{-2}$) inferred from burning experiments [28] and was estimated

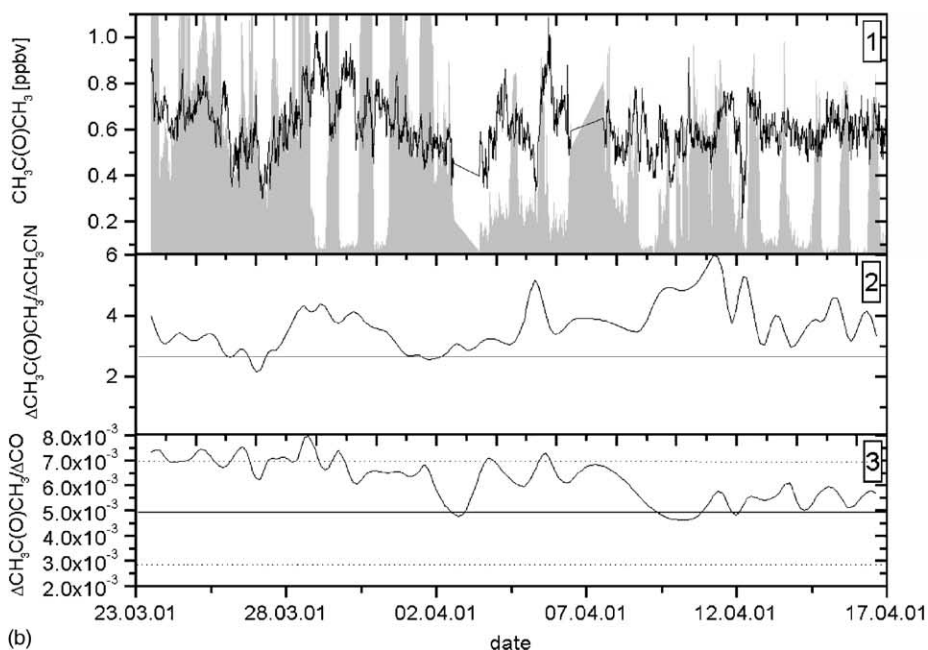
for a 10-day-old air parcel assuming an average HO density (ca. 25% of maximum concentration) of 1×10^6 molecules/cm³ [27] and a reaction constant with HO of $k_{\text{HO}}^{298} = 9.3 \times 10^{-13}$ cm³/molecule s [21] for methanol and $k_{\text{HO}}^{298} = 2.1 \times 10^{-13}$ cm³/molecule s for CO [21]. This is significantly lower than the observed ratios. Methanol to acetonitrile ratios were significantly higher ($\Delta\text{CH}_3\text{OH}/\Delta\text{CH}_3\text{CN} = 5\text{--}14$) than estimates from biomass burning experiments ($\Delta\text{CH}_3\text{OH}/\Delta\text{CH}_3\text{CN} = 2.2 \pm 3$) [28]; our observations, therefore, suggest that the ambient mixing ratios were not greatly influenced by biomass burning. Methanol, an ubiquitous species in the atmosphere, has many sources. Global emission inventories reflect the fact that measurements of this compound are still very scarce [29]. To our knowledge, this was the first time that ambient mixing ratios of methanol were measured on Mauna Loa for a 4-week period. Singh et al. [5] speculate that there might be large primary sources from biogenic emissions. Indeed, first results from several flux studies [51] show high methanol emission rates on the order of several mg/m² h. The biogenic source [30] and emission from dead/decaying plant matter [31] of methanol is probably far bigger than secondary production from methane/NMHC oxidation ($2\text{CH}_3\text{O}_2 \rightarrow \text{CH}_3\text{OH} + \text{O}_2$, 30 Tg/year). Heikes et al. [29] estimate 320 Tg of methanol per year released by biogenic activities. Biomass burning and oceanic sources are thought to be the second major global sources for methanol estimated to account for as much as 22% of the total [29].

3.4. Acetone

Interest in acetone ($k_{\text{HO}}^{298} = 1.9 \times 10^{-13}$ cm³/molecule s [21]) comes from its potential importance in the upper troposphere, where acetone oxidation can produce HO_x radicals (HO + HO₂) [32] and thus contribute to ozone formation [33,34]. Acetone can also act as an intermediate sink for NO_x radicals (NO + NO₂) by forming peroxy-acetyl nitrate (PAN) and transport these radicals over long distances. Highly variable acetone mixing ratios have been observed in several previous field studies. Arnold et al.



(a)



(b)

Fig. 2. (a) Panel 1: methanol mixing ratios plotted together with relative humidity (shaded area); panel 2: correlation coefficient r between methanol and CO; panel 3: $\Delta\text{CH}_3\text{OH}/\Delta\text{CO}$ ratios, the straight line indicates emission ratios from biomass burning. Correlation coefficients and $\Delta\text{CH}_3\text{OH}/\Delta\text{CO}$ ratios were calculated on an 8-h running mean basis. (b) Panel 1: acetone mixing ratios plotted together with relative humidity (shaded area); panel 2: $\Delta\text{CH}_3\text{COCH}_3/\Delta\text{CO}$ ratios; panel 3: $\Delta\text{CH}_3\text{COCH}_3/\Delta\text{CH}_3\text{CN}$ ratios; straight solid lines indicate emission ratios from biomass burning, dashed lines reflect the observed variability. $\Delta\text{CH}_3\text{COCH}_3/\Delta\text{CO}$ and $\Delta\text{CH}_3\text{COCH}_3/\Delta\text{CH}_3\text{CN}$ ratios were calculated on an 8-h running mean basis. (c) Panel 1: acetonitrile mixing ratios plotted together with relative humidity (shaded area); panel 2: correlation coefficient r between acetonitrile and CO; panel 3: $\Delta\text{CH}_3\text{CN}/\Delta\text{CO}$ ratios, the straight solid line indicates emission ratios from biomass burning, dashed lines reflect the observed variability. Correlation coefficients and $\Delta\text{CH}_3\text{CN}/\Delta\text{CO}$ ratios were calculated on an 8-h running mean basis.

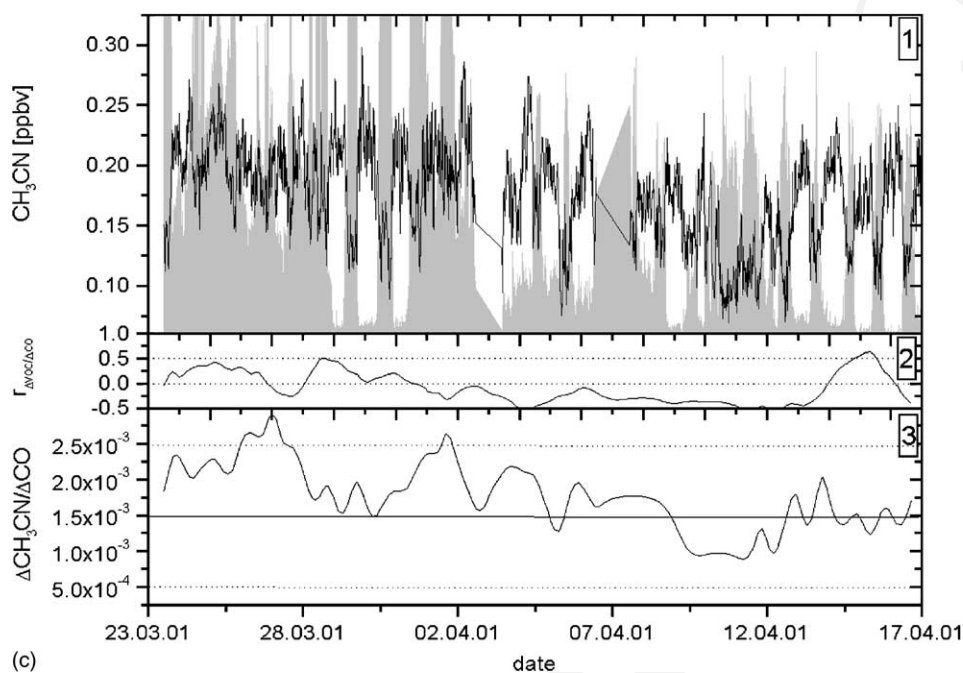


Fig. 2. (Continued).

325 [35] report 3 ppbv in the upper troposphere in the
 326 North Atlantic flight corridor, similar enhanced con-
 327 centrations (2.6 ± 1 ppbv) above the tropical rainforest
 328 were published by Pöschl et al. [36], whereas much
 329 smaller values around 100 pptv were found in the Pa-
 330 cific region during PEM-West (Pacific Exploratory
 331 Mission) [33]. de Gouw et al. [9] report mixing ra-
 332 tios around 500 pptv at altitudes between 4–12 km and
 333 2000 pptv in the lower troposphere (<3 km) during
 334 the INDOEX. Clean background concentrations in the
 335 pristine boundary layer of the Indian Ocean were ob-
 336 served to be around 450 [6], 350 [7], and 300–800 pptv
 337 [37].

338 In this study, acetone concentrations ranged be-
 339 tween 200 and 1000 pptv (Fig. 2b). In contrast to
 340 methanol, isoprene, MVK + MACR, and acetonitrile,
 341 the averaged diurnal acetone profile (Fig. 1, panel 6)
 342 shows no clear trend. Enhanced levels were found dur-
 343 ing downslope conditions on March 29 (1000 pptv),
 344 30 (800 pptv), and 31 (600 pptv), when 10-day back-
 345 trajectories suggest a shift from SE to NE winds.
 346 The mean acetone concentration 600 ± 200 pptv was

close to values reported by Greenberg et al. [38] dur-
 347 ing the MLOPEX 2 study. $\Delta\text{CH}_3\text{COCH}_3/\Delta\text{CO}$ ratios
 348 (Fig. 2b, panel 3) around 7×10^{-3} with reasonably
 349 high correlation coefficients (0.5–0.8) occurred during
 350 the first part of the study (March 23–April 2) and were
 351 lower ($\Delta\text{CH}_3\text{COCH}_3/\Delta\text{CO} = 5 \times 10^{-3}$) from April
 352 12 onwards. Emission factors from biomass burning
 353 would predict values in the range of $4.6 \pm 2.7 \times 10^{-3}$
 354 as indicated by the straight lines in Fig. 2b (panel 3).
 355 Correlation coefficients from April 12 onwards show
 356 significant variation, with r close to 0 during day-
 357 time upslope and r around 0.5–0.8 during nighttime
 358 downslope winds; the higher correlation in free tropo-
 359 spheric airmasses can be rationalized by common
 360 acetone and CO sources on a larger scale. This is also
 361 supported by the cross spectrum of acetone and CO,
 362 which shows that most of the positive cross correlation
 363 occurs on a time scale around ~ 5 –10 days; wavelet
 364 analysis (using the morlet wavelet; $k = 6$) [55] re-
 365 vealed that this mode was dominant throughout almost
 366 the whole measurement period; superimposed a sec-
 367 ond mode on a 1–2 day basis reflected differences in
 368

369 diurnal variations. Acetonitrile can be regarded as a
 370 reasonably good marker for biomass burning. Emission
 371 factors for Δ acetone/ Δ acetonitrile have been reported
 372 for direct emissions (3.1–5.8 ppbv/ppbv, corrected for a
 373 \sim 10-day-aged air mass from [28]) and processed plumes
 374 (16.2–20 ppbv/ppbv) [39]. Values measured at the MLO are
 375 closer to the primary emissions (2–5 ppbv/ppbv) and are
 376 shown in Fig. 2b (panel 3). Peak values (8–9 ppbv/ppbv) are
 377 typically related to upslope winds and/or poor correlation
 378 coefficients. Highest coefficients were observed on March 29
 379 ($r = 0.85$), 30 ($r = 0.5$), and April 14 ($r = 0.5$).

381 3.5. Acetonitrile

382 Acetonitrile ($k_{\text{HO}}^{298} = 2.2 \times 10^{-14} \text{ cm}^3/\text{molecule s}$
 383 [21]) is thought to be primarily released from biomass
 384 burning, although minor contributions from fossil
 385 fuel emissions (<6% [40,41]) and biogenic emissions
 386 from the breakdown of cyanogenic glycosides similar to
 387 HCN might exist [42]. Tropospheric background
 388 measurements were reported in the range of

0.075–0.2 ppbv for remote areas and up to 0.4 ppbv
 389 in polluted regions during the INDOEX study [6,37].
 390 Warneke and de Gouw [7] measured 122, 154, and
 391 145 pptv in the Southern and Northern Indian Ocean
 392 and the Gulf of Aden, respectively. Mixing ratios on
 393 ML during Spring 2001 showed minimum concentrations
 394 around 70 pptv and peak values up to 300 pptv.
 395 This fits well within the previously published concentration
 396 range (Fig. 2b, panel 1).
 397

The lifetime according to the reaction with HO radicals
 398 is \sim 912 days assuming an average HO density of
 399 $1 \times 10^6 \text{ molecules/cm}^3$. This does not agree well with
 400 observed variability trends [6], which suggests a much
 401 lower lifetime. de Laat et al. [10] need an ocean sink
 402 assuming dry deposition velocities of 0.01–0.05 cm/s
 403 in order to fit modeled acetonitrile data to mixing
 404 ratios measured during the INDOEX campaign; however,
 405 state that stratosphere/troposphere exchange was not
 406 included in their ECHAM (European Center for
 407 Medium Range Weather Forecasting) model. Wet
 408 deposition of acetonitrile through rain out is currently
 409 thought to play a minor role [43,44]. Fig. 3 shows a

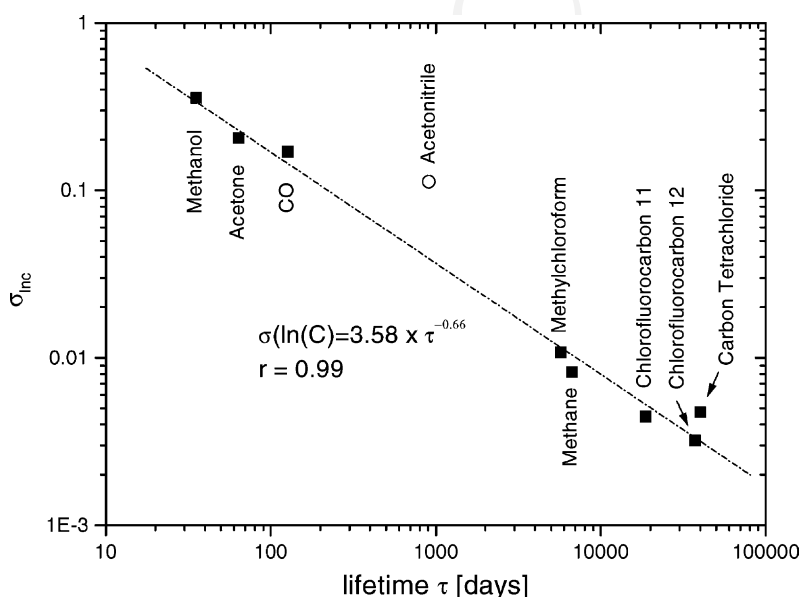


Fig. 3. Variability–lifetime plot of methanol, acetone, acetonitrile, CO, CH₄, methylchloroform, chlorofluorocarbon 11 (F11), chlorofluorocarbon 12 (F12), and carbon tetrachloride. Lifetimes were calculated according to reaction losses due to photolysis and HO radicals. Troposphere Stratosphere Exchange was not considered.

410 variability–lifetime plot ($s_{\text{lnc}} = A\tau^{-b}$) for some se-
 411 lected long-lived species. The straight line ($r = 0.99$)
 412 was fitted through all compounds except acetonitrile.
 413 The b factor (0.66) which can be considered as an
 414 age factor (the more distant to potential sources the
 415 higher) [45,46] is rather large close to values reported
 416 during INDOEX (0.4 [7]), PEM-West (0.54 [45]),
 417 and LBA-Claire (Large Scale Biosphere-Atmosphere
 418 Experiment in Amazonia) (0.64 [47]). The A coef-
 419 ficient (3.58) can be interpreted as a range factor for
 420 sampled air mass ages. The observed value (3.58)
 421 in Fig. 4 is comparable to those measured during
 422 LBA-Claire (4.63) [47] and PEM-West B (4.3) [45]
 423 and indicates a rather large age range of sampled
 424 pollutants. It is obvious that acetonitrile does not lie
 425 within the normal trend ($\tau = 912$ days) if the only
 426 considered sink is loss due to reaction with HO rad-
 427 icals. Instead, a lifetime of $\tau = 183$ days seems to be
 428 more realistic. The high variability is mainly caused

429 by a pronounced diurnal profile showing lower mixing
 430 ratios during upslope (140 pptv) and higher mixing
 431 ratios during downslope conditions (200 pptv) (Fig. 1,
 432 panel 7). Extreme events caused diurnal variations up
 433 to a factor of 2 (March 29–31, April 13–17). These
 434 observations seem to support the idea of a missing
 435 sink or polluted layers transported by the aloft. Can
 436 the pronounced concentration gradient between ma-
 437 rine boundary layer (upslope) and free tropospheric
 438 air (downslope) be explained by an ocean sink?

439 Statistical analysis (Fig. 4) of the concentration dif-
 440 ferences δC in up- and downslope conditions during
 441 the Mauna Loa Spring 2001 experiment can be used
 442 to test, if the mean gradient seen between the mixed
 443 layer and the free troposphere is due to an uptake in
 444 ocean water. Using a steady-state approach and the
 445 typical marine, convective boundary layer structure,
 446 the concentration jump (ΔC) at the top of the bound-
 ary layer should be proportional to the ratio of dry

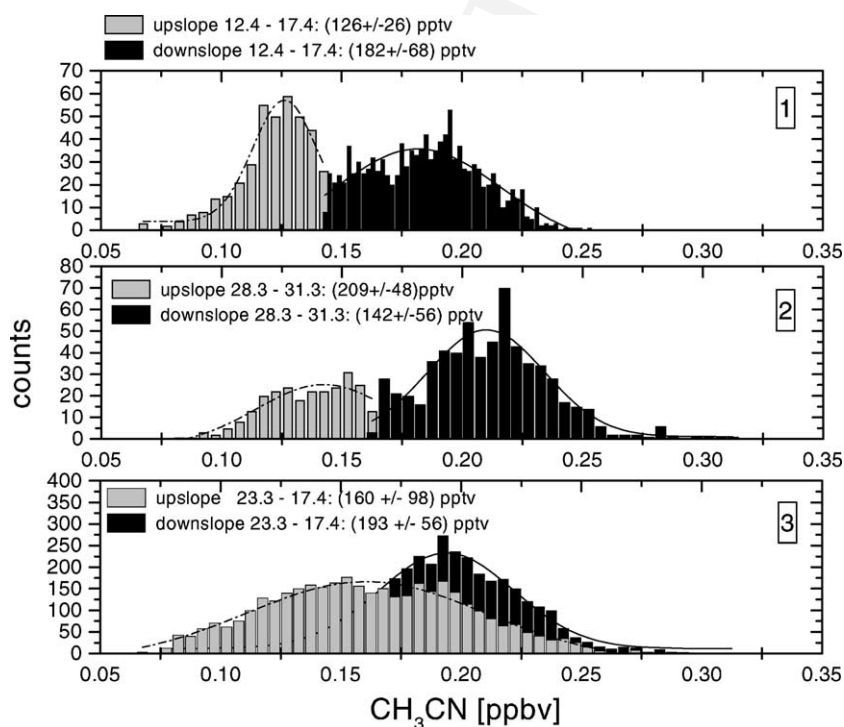


Fig. 4. Acetonitrile concentrations in up- and downslope conditions for the whole MLO Spring 2001 dataset (March 23, 2001–April 17, 2001) and two subsets (March 29, 2001–March 31, 2001 and April 12, 2001–April 17, 2001).

Table 1

Estimated (est.) and experimental (exp.) acetonitrile deposition velocities (v_d) from the literature compared with values obtained from this work (v_e , entrainment velocity in cm/s)

| Reference | Reported v_d (cm/s) | Comments | Method |
|--|--|---|--------|
| [52] | 1×10^{-3} to 3×10^{-3} | Estimation using molecular diffusivities | est. |
| [53] | 0.04–3.7 | Adopted from HCN: $v_d \sim u^2$; used in Harvard Global Model | est. |
| [54] | 0.05 | Parameterized resistances | est. |
| [10] | 0.01–0.05 | New parametrization according to experimental data from the INDOEX 1999 | exp. |
| MLO 2001 | | | v_e |
| March 28, 2001–April 17, 2001 | 0.10 | Downslope: 19:00–7:00 | 0.5 |
| March 23, 2001–April 28, 2001 and April 1, 2001–April 14, 2001 | 0.09 | Downslope: 19:00–7:00 | 0.5 |
| March 28, 2001–March 31, 2001 | 0.24 | Downslope: 19:00–7:00 | 0.5 |
| April 14, 2001–April 17, 2001 | 0.17 | Downslope: 19:00–7:00 | 0.5 |

447 deposition and entrainment velocities. A simple form
448 of the mixed layer can be written as,

$$449 \frac{\partial C}{\partial t} + U \frac{\partial C}{\partial x} + \frac{\overline{w}c_{zi} - \overline{w}c_s}{z_i} = S \Rightarrow \frac{\Delta C}{C_{ml}} = \frac{v_d}{v_e} \quad (2)$$

450 with C (mixing ratio), C_{ml} (concentration in the mixed
451 layer), U (horizontal wind speed), wc_{zi} (entrainment
452 flux), wc_s (surface flux), z_i (boundary layer height),
453 S (chemical loss term), v_d (deposition velocity) and
454 v_e (entrainment velocity). Taking typical values for
455 v_e (0.5 cm/s) measured above the remote ocean [48]
456 and data obtained from this study, we find that the
457 mean gradient could be caused by v_d of 0.1 cm/s for
458 the average concentration profile during the whole
459 study and 0.24 and 0.17 cm/s during March 29–31
460 and April 13–17, respectively. Table 1 shows a com-
461 parison with data for v_d from the literature. Compared
462 to model results from de Laat et al. [10], the mean
463 v_d (0.1 cm/s) is higher by a factor of 2. Two peri-
464 ods (March 29, 2001–March 31, 2001 and April 13,
465 2001–April 17, 2001) were characterized by a sig-
466 nificant enhancement of free tropospheric acetonitrile
467 concentrations resulting in at least five times higher
468 deposition velocities. Even if an uncertainty for en-
469 trainment velocities by a factor of two is considered,
470 these enhanced free tropospheric concentrations can-
471 not only be explained by dry deposition in steady
472 state. Remote sensing data (World Fire Web [49])

473 show that extensive vegetation fires in South-East
474 Asia and the Indian Subcontinent occurred during
475 March and April 2001. Backtrajectories from April
476 13–16 point westward towards these regions. This
477 supports the idea of air masses influenced by biomass
478 burning which were transported across the Pacific
479 by the aloft within 5–10 days and had not entirely
480 reached an equilibrium with lower marine boundary
481 layer air.

482 The correlation between CH_3CN and CO is shown
483 in Fig. 2c (panel 3). The ratios range from 1.0 to
484 2.7×10^{-3} . The period from April 13 on is charac-
485 terized by $\Delta\text{CH}_3\text{CN}/\Delta\text{CO}$ ratios around 1.5×10^{-3}
486 during downslope conditions falling close to values
487 reported for biofuel ($1.5 \pm 1.0 \times 10^{-3}$, corrected for
488 a ~ 10 -day-aged air mass from [28]). The correlation
489 coefficients $r_{\text{CH}_3\text{CN}/\text{CO}}$ were reasonably high, around
490 0.6, 0.5, and 0.7 on March 24, March 29–30, and April
491 14–15, respectively.

4. Conclusion 492

493 Continuous ground-based measurements of acetonitrile,
494 acetone, methanol, isoprene, and MVK + MACR
495 made with a Proton-Transfer Reaction Mass Spec-
496 trometer were performed at the Mauna Loa Baseline
497 Observatory (CMDL, NOAA) in Spring 2001.

498 Local influence from the islands caused elevated
 499 concentrations for some biogenic and/or oceanic
 500 VOCs, such as isoprene, its oxidation products
 501 MVK + MACR and sometimes methanol, during af-
 502 ternoon upslope conditions with mean concentrations
 503 of 30 pptv, 100 pptv, and 1 ppbv, respectively. Ace-
 504 tonitrile, acetone, and CO were highly correlated on
 505 scales between 5 and 7 days during March and the be-
 506 ginning of April (March 23, 2001–April 2, 2001); on
 507 March 29–31 specifically, high correlation between
 508 these compounds can be rationalized by the back-
 509 trajectories suggesting that air masses were passing
 510 the Pacific in northern latitudes and shifting ‘back’
 511 south-east before hitting the US West coast. Influe-
 512 nce from both, the Asian continent and the western
 513 part of the US is likely. Acetone levels in these cases
 514 (0.2–1 ppbv) showed reasonably high correlation with
 515 CO ($\Delta\text{CH}_3\text{COCH}_3/\Delta\text{CO} \sim 7 \times 10^{-3}$; $r = 0.8$).
 516 Highly variable and enhanced free tropospheric ace-
 517 tonitrile concentrations, a marker for biomass burning
 518 and domestic fuel, suggest that the site was partly
 519 influenced by biomass burning activities. Detailed
 520 backtrajectory analysis showed that between April 13
 521 and 17 air masses from South-East Asia and the In-
 522 dian Subcontinent were transported across the Pacific
 523 within a week resulting in a distinct concentration gra-
 524 dient between marine boundary layer and free tropo-
 525 spheric air. Correlation coefficients between CO and
 526 acetonitrile up to 0.7 ($\Delta\text{CH}_3\text{CN}/\Delta\text{CO} = 1.5 \times 10^{-3}$)
 527 suggest further that part of the observed CO mixing
 528 ratios originated from biomass burning activities such
 529 as direct emission and secondary formation in VOC
 530 enriched plumes.

531 Acknowledgements

532 This paper is dedicated to the memory of our col-
 533 league, mentor, and friend Prof. Dr. Werner Lindinger,
 534 who lost his life in a tragic accident on Hawaii at
 535 the beginning of this experiment in February 2001.
 536 Financial support came from the Austrian Fond
 537 zur wissenschaftlichen Foerderung (FWF) project
 538 14170, the Bundesministerium für Bildung, Kunst

und Forschung, Wien, Austria, the Climate Monitor- 539
 ing and Diagnostics Laboratory (NOAA), and NOAA 540
 Grant No. NA06GP0483. 541

T.K. was also supported by the Atmospheric Chem- 542
 istry Division and the Advanced Study Program at the 543
 National Center for Atmospheric Research. The Na- 544
 tional Center for Atmospheric Research is sponsored 545
 by The National Science Foundation. The authors also 546
 want to express thanks to Carsten Warneke, Joost de 547
 Gouw, and Brian Heikes for sharing unpublished re- 548
 sults, Claire Granier and Guy Brasseur for helpful dis- 549
 cussions and Russ Schnell, Fred Fehsenfeld, Ray Fall, 550
 and Alex Guenther for their support. 551

References 552

- [1] U.K. Sharma, Y. Kajii, H. Akimoto, *GRL* 27 (2000) 2505. 553
- [2] R.E. Newell, M.J. Evans, *GRL* 27 (2000) 2509. 554
- [3] CMDL, NOAA, Annual Meeting, Abstracts, Boulder, 2001. 555
- [4] K.E. Wilkening, L.A. Barrie, M. Engle, *Science* 290 (2000) 556
xx. 557
- [5] H.B. Singh, Y. Chen, A. Staudt, D. Jacob, D. Blake, B. 558
Heikes, J. Snow, *Nature* 410 (2001) 1078. 559
- [6] A. Wisthaler, A. Hansel, R.R. Dickerson, P.J. Crutzen, J. 560
Geophys. Res.-Atmospheres, submitted for publication. 561
- [7] C. Warneke, J.A. de Gouw, *Atmos. Environ.* 35 (2001) 5923. 562
- [8] J. Lelieveld, et al., *Science* 291 (2001) 1031. 563
- [9] J.A. de Gouw, C. Warneke, H.A. Scheeren, C. van der Veen, 564
M. Bolder, M.P. Scheele, J. Williams, S. Wong, L. Lange, H. 565
Fischer, J. Lelieveld, *J. Geophys. Res.* 106 (2001) 28469. 566
- [10] A.T.J. de Laat, J.A. de Gouw, J. Lelieveld, A. Hansel, *JGR* 567
(2001) 28469. 568
- [11] W. Lindinger, A. Hansel, A. Jordan, *IJMS* (1998) 191. 569
- [12] T. Karl, R. Fall, P.J. Crutzen, A. Jordan, W. Lindinger, *GRL* 570
(2001) 507. 571
- [13] J.A. de Gouw, C. Warneke, T. Karl, G. Eerdekens, C. van 572
der Veen, R. Fall, *IJMS*, this issue. 573
- [14] R.R. Draxler, G.D. Hess, *Aust. Met. Mag.* (1998) 295. 574
- [15] J.M. Harris, J.D. Kahl, *JGR* (1990) 13651. 575
- [16] J.R. Parrington, W.H. Zoller, N.K. Arras, *Science* (1983) 195. 576
- [17] S.J. Oltmans, H. Levy II, *Atmos. Environ.* (1994) 9. 577
- [18] T.A. Schroeder, *J. Appl. Meteorol.* (1981) 874. 578
- [19] B.G. Mendonca, *J. Appl. Meteorol.* (1969) 533. 579
- [20] J.G. Walega, B.A. Ridley, S. Madronich, F.E. Grahek, J.D. 580
Shetter, T.D. Sauvain, C.J. Hahn, J.T. Merill, B.A. Bodhaine, 581
E. Robinson, *JGR* (1992) 10311. 582
- [21] IUPAC, Summary of Evaluated Kinetic and Photochemical 583
Data for Atmospheric Chemistry, Web Version December 584
2000. Available at: <http://www.iupac-kinetic.ch.cam.ac.uk>. 585
- [22] P. Harley, V. Fridd-Stroud, J. Greenberg, A. Guenther, P. 586
Vasconcellos, *JGR* (1998) 25479. 587

- 588 [23] P.D. Goldan, W.C. Kuster, F.C. Fehsenfeld, S.A. Montzka,
589 JGR (1993) 1039. 620
- 590 [24] J.P. Greenberg, P.R. Zimmerman, W.F. Pollock, R.A. Lueb,
591 L.E. Heidt, JGR (1992) 10395. 622
- 592 [25] P.J. Milne, D.D. Riemer, R.G. Zika, L.E. Brand, Mar. Chem.
593 (1995) 237. 624
- 594 [26] D. Helmig, W. Pollock, J.P. Greenberg, P. Zimmerman, JGR
595 (1996) 14697. 626
- 596 [27] F.L. Eisele, D.J. Tanner, C.A. Cantrell, J.G. Calvert, JGR
597 (1996) 14665. 628
- 598 [28] R. Holzinger, C. Warneke, A. Hansel, A. Jordan, W.
599 Lindinger, D.H. Scharffe, G. Schade, P.J. Crutzen, GRL
600 (1999) 1161. 630
- 601 [29] G.B. Heikes, W. Chang, M.E.Q. Pilson, E. Swift, H.B. Singh,
602 A. Guenther, D.J. Jacob, B.D. Field, R. Fall, D. Riemer, L.
603 Brand, JGR, submitted for publication. 632
- 604 [30] R. Fall, A.A. Benson, Trends Plant Sci. (1996) 296. 633
- 605 [31] C. Warneke, T. Karl, H. Judmaier, A. Hansel, A. Jordan, W.
606 Lindinger, P.J. Crutzen, Global Biogeochem. Cycles (1999)
607 9. 634
- 608 [32] H.B. Singh, M. Kanakidou, P.J. Crutzen, D.J. Jacob, Nature
609 (1995) 50. 635
- 610 [33] S.A. McKeen, et al., GRL (1997) 3177. 636
- 611 [34] P. Wennberg, Science (1998) 49. 637
- 612 [35] F. Arnold, V. Bürger, B. Drostefanke, F. Grimm, A. Krieger,
613 J. Schneider, T. Stulp GRL (1997) 3017. 638
- 614 [36] U. Pöschl, U.J. Williams, P. Hoor, H. Fischer, P.J. Crutzen, C.
615 Warneke, R. Holzinger, A. Hansel, A. Jordan, W. Lindinger,
616 H.A. Scheeren, W. Peters, J. Lelieveld, J. Atmos. Chem.
617 (2001) 115. 639
- 618 [37] D. Sprung, C. Jost, T. Reiner, A. Hansel, A. Wisthaler, JGR
619 (2001) 28511. 640
- [38] J.P. Greenberg, D. Helmig, P.R. Zimmerman, JGR (1996) 620
24581. 621
- [39] A. Andreae, et al., GRL (2001) 951. 622
- [40] R. Holzinger, A. Jordan, A. Hansel, W. Lindinger, J. Atmos.
623 Chem. (2001) 187. 624
- [41] Bange, J. Williams, Atmos. Environ. (2000) 4959. 625
- [42] R. Fall, T.G. Custer, S. Kato, V. Bierbaum, Atmos. Environ.
626 (2001) 1713. 627
- [43] S. Hamm, P. Warneke, JGR (1990) 20593. 628
- [44] E. Arijs, G. Brasseur, JGR (1986) 4003. 629
- [45] B.T. Jobson, S.A. McKeen, D.D. Parrish, F.C. Fehsenfeld,
630 D.R. Blake, A.H. Goldstein, S.M. Schauffler, J.W. Elkins,
631 JGR (1999) 16090. 632
- [46] T. Karl, P.J. Crutzen, M. Mandl, M. Staudinger, A. Guenther,
633 A. Jordan, R.F.W. Lindinger, Atmos. Environ. (2001) 5287. 634
- [47] J. Williams, H. Fischer, G.W. Harris, P.J. Crutzen, P. Hoor, A.
635 Hansel, R. Holzinger, C. Warneke, W. Lindinger, B. Scheeren,
636 J. Lelieveld, JGR (2000) 20473. 637
- [48] R. Boers, P.B. Krummel, S.T. Siems, G.D. Hess, JGR (1998)
638 16637. 639
- [49] <http://www.gvm.sai.jrc.it>. 640
- [50] <http://www.science.sp-agency.ca/J1-MOPITT>. 641
- [51] T. Karl, C. Spirig, P. Prevost, C. Stroud, J. Rinne, J.
642 Greenberg, R. Fall, A. Guenther, personal communication. 643
- [52] R.P. Schwarzenbach, P.M. Gschwend, D.M. Imboden,
644 Handbook for Environmental Organic Chemistry, Wiley, New
645 York, 1993. 646
- [53] Q. Li, D.J. Jacob, I. Bey, R.M. Yantosca, Y. Zhao, Y. Kondo,
647 J. Notholt, GRL (2000) 357. 648
- [54] M.L. Wesley, Atmos. Environ. (1989) 1293. 649
- [55] C. Torrence, G.P. Compo, Bull. Am. Meteorological Soc.
650 (1997) 61. 651